

Lateral Force and Turning Moment on a Reversing Ship

Lucia Sileo¹, Sverre Steen²

¹Norwegian Marine Technology Research Institute (MARINTEK), Trondheim, Norway (*)

²Department of Marine Technology, Norwegian University of Science and Technology (NTNU), Trondheim, Norway

ABSTRACT

The current work investigates, both with model tests and numerical calculations, the forces and turning moments experienced by a single-screw ship model in reversing mode. Model tests were carried out by Marintek, in the large towing tank of the Marine Technology Center in Trondheim, on a chemical tanker model. RANS calculations were then carried out also considering additional conditions with respect to the model tests. The ship length was also modified in order to investigate how this parameter, as well as ship speed and propeller loading, can affect the forces and moments experienced by the model. The main goal was to provide data and physical understanding about the hydrodynamic reasons which prevent a reversing single-screw ship from traveling straight backward, determining, instead, a side rotation. A complementary scope was to develop a simplified model suited for implementation in a real-time ship simulator.

Keywords

Reversing ship, RANS

1 INTRODUCTION

Sophisticated engineering tools are increasingly applied, not only for designing ships and ship equipment, but also for planning of operations and training of crew, like ship simulators. Low speed maneuvers are important cases to handle, and their prediction of maneuverability is very challenging because of non-linear effects caused by complex interactions between propeller and hull. For instance, it is known that when a ship is reversing, it will not travel straight backwards, but turn sideways. In fact, at low speed, in addition to the given propeller thrust acting as a direct steering force, indirect steering forces are created as interaction effects between the propeller jet and the adjacent ship hull. The pressure field induced on the hull by the astern running propeller normally produces indirect transverse forces in vicinity of the stern, which increase with the propeller thrust (Brix 1993).

The current work investigates, both with model tests and numerical calculations, forces and turning moments experienced by a ship model in reversing mode. Model tests were carried out by Marintek in March 2010 on a chemical tanker model with a “Promas” propulsion unit designed by Rolls-Royce. Three test cases were considered: the negative ship advance velocity was kept constant in all cases, while the propeller revolutions were reduced from Test1 to Test3 as described in Tab. 1.

Table 1: Tests description.

Test1	Test2	Test3
P_{rev1} [rps]	P_{rev2} [rps]	P_{rev3} [rps]
-8.14	-6.11	-4.07

In a second stage, additional tests were performed by numerical calculations only, keeping the propeller conditions like in Test1 and Test3, but reducing the ship velocity by 50%. The new tests are respectively named Test11 and Test13. Then all the calculations, except Test2, were repeated on a modified model; the original mid hull, which is the part with parallel side walls, was shortened by 90% of its length. Both models are shown in Fig. 1. The main scope was to quantify the variations of turning moment on the model resulting from changing the advance velocity and/or the ship length. The test cases for the modified model have the letter M in addition to the previous test names.

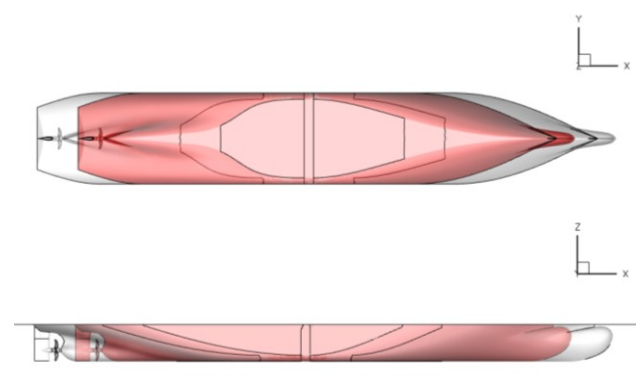


Figure 1: Original and modified ship model.

(*) Formerly Department of Marine Technology, Norwegian University of Science and Technology (NTNU), Trondheim, Norway

2 NUMERICAL MODELLING

The double-precision pressure-based incompressible Fluent solver was used to solve the 3D RANS equations, with the SST $k-\omega$ model for turbulence closure (Menter 1994). Second order discretization schemes were used to solve the convective terms in all the equations, and the SIMPLE algorithm was used for the pressure correction equation. The computational domain is described in Fig. 2, together with the boundary conditions. The free surface is considered frictionless and without deformation.

The hybrid mesh is composed of about six million cells, with 8 layers of hexahedral cells attached to the wall surfaces, while the remaining volume is filled with tetrahedral cells. The rotating wall surfaces, i.e., the propeller blades and hub, are embedded in a separate zone of the volume mesh, as shown in Fig. 3, with a detail of the mesh at the stern.

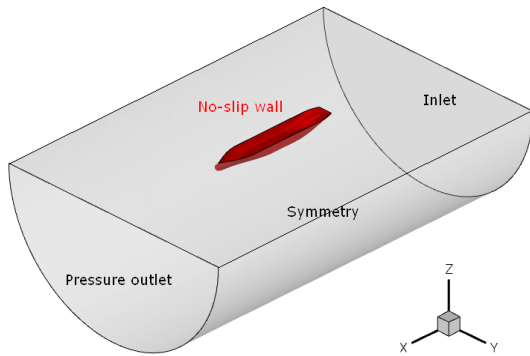


Figure 2: Computation domain with boundary conditions.

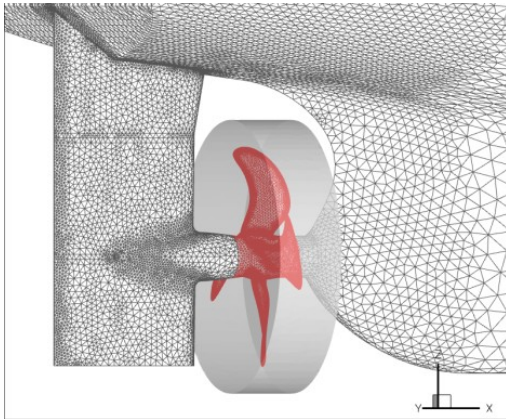


Figure 3: Detail of the mesh at the stern.

This secondary fluid zone can rotate together with the propeller with constant speed or it can be defined as a relative reference frame in which the non-inertial equations of motion are solved in terms of the relative velocity. These two different approaches are called Sliding Mesh (SM) and Multi Reference Frame (MRF) (Fluent, 2006), respectively. In the present case, the MRF was used at first to save computational efforts, as it is less computationally demanding, and to have an initial guess of the flow field for the following transient calculations with the SM approach. To capture the unsteady flow features and to have a more accurate description of the flow, the SM approach was then used afterward. The time

step for the transient calculations was varied from 0.001 to 0.002 [sec] so that it is equivalent to 3 degrees of propeller rotation for each case.

3 VALIDATION OF RESULTS

Validation is made through the comparison of numerical results against model test data, in terms of propeller thrust and torque and lateral force and turning moment acting on the overall ship model. Numerical results are in very good agreement with model tests, in terms of averaged values, as shown in Fig. 4, as well as in terms of time series. Both in calculations and model tests, the increase of propeller loading results in an increase of total turning moment, which is negative in the adopted reference system, i.e., the stern of the ship would rotate from starboard to port. In fact, the flow downstream the propeller has a tangential velocity component induced by the propeller rotation, and the ship tends to rotate so that it will get aligned with the flow, as shown by the volume streamlines in Fig. 5.

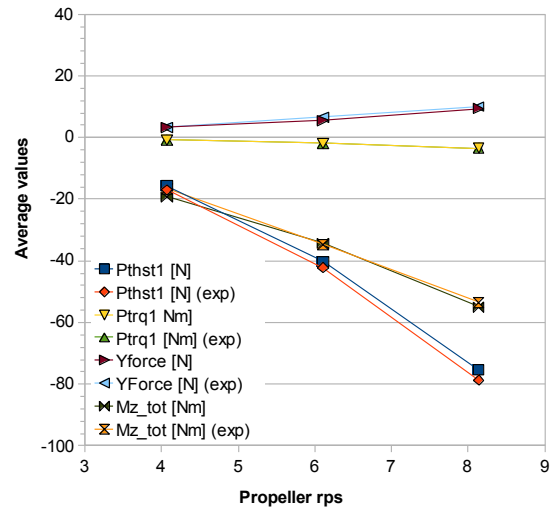


Figure 4: Results validation. Propeller thrust and torque and total lateral force and turning moment. Average values.

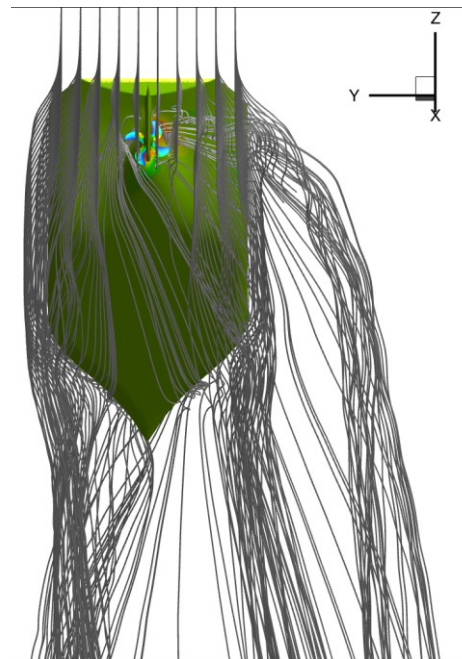


Figure 5: Volume streamlines.

4 PRESSURE DISTRIBUTION AND INDIRECT PROPELLER FORCES

Pressure contours at the starboard and port side of the model have a non-symmetric distribution, especially at the aft. In fact, zooming in on the stern, in Fig. 6, a large area of high pressure is visible only on the starboard side, at the aft end of the hull, immediately downstream and above the propeller. This suggests that the propeller slipstream is pushed against the hull with a tangential component, i.e., with a non-zero angle of attack. In this situation, the hull acts like a big rudder with a non-zero angle of incidence, experiencing on the stern a lateral force from starboard to port which causes a negative yaw moment on the overall ship model. The non-symmetric pressure distribution produces a positive (to port) lateral force at the stern, where the SB side shows a higher pressure than the PT side. Note that the propeller was

right handed; in reversing condition, the rotation direction is therefore anti-clockwise when seen from the stern looking toward bow.

The bow, on the other hand, is affected by a lateral force in the negative (to starboard) direction. In fact, adjusting the pressure contour levels it is possible to point out the asymmetries between PT and SB side in the fore part of the model, as illustrated in Fig. 7. The area of negative pressure on the SB side is larger and shows lower minimum value with respect to PT side, while a high pressure area is confined in a small region in the upper part of the fore hull. As a consequence, the fore part of the model experiences a negative lateral force, i.e., from PT to SB. The value of these forces depends on test conditions and presumably by the ship geometry. This is discussed in the next section.

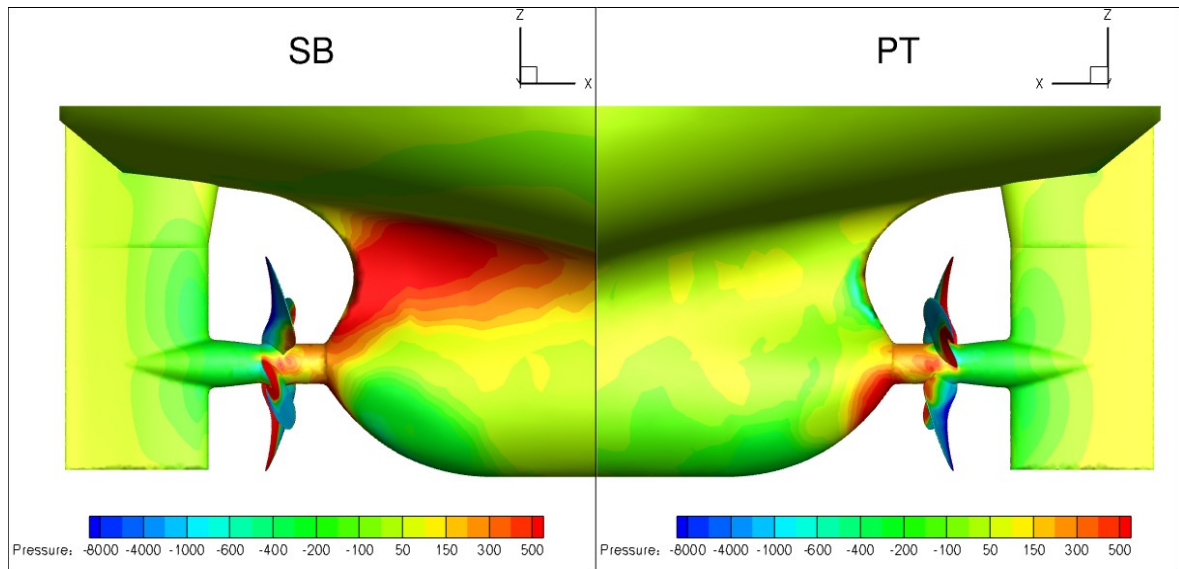


Figure 6: Test1. Pressure contours of static pressure on the starboard and port side of the stern.

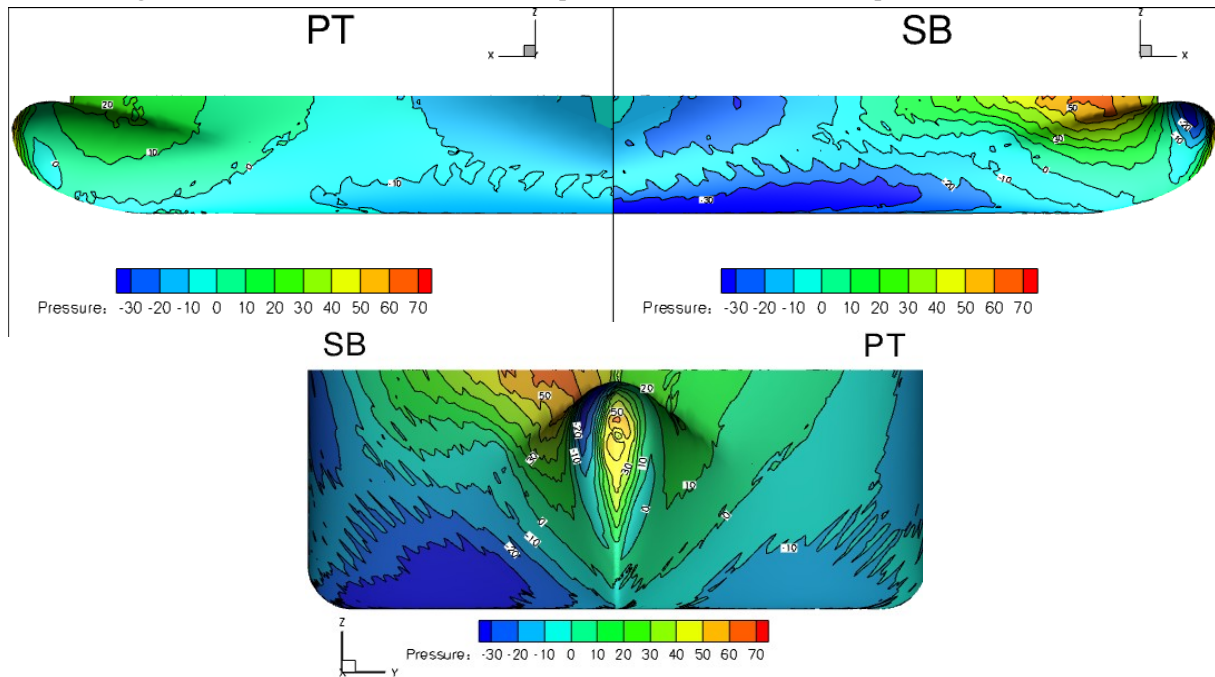


Figure 7: Test1. Pressure contours of static pressure on the starboard and port side of the forehead.

5 NEW SHIP VELOCITY AND SHIP LENGTH

Analyses of the numerical results obtained for all the test conditions and for the two different ship models show that the propeller thrust and torque are not affected by the ship length, but they slightly increase in their absolute value when the ship velocity is decreased, keeping the same propeller revolution; this could be expected because of the reduction of the advance ratio. In fact, thrust and torque coefficients K_T and K_Q do not change when considering test cases with the same advance ratio.

Forces and moments acting on the model are reported below in non-dimensional form; forces are made non-dimensional by dividing by the absolute value of propeller thrust T [N], while moments are made non-dimensional by dividing by the absolute value of propeller thrust times the ship length L_{PP} [m]. Time is made non-dimensional by multiplying with the axial velocity at the propeller disc $(V_s + U_a/2)$ [ms^{-1}] and dividing by L_{PP} . V_s is the ship advance velocity and U_a is the induced axial velocity, which was estimated applying the momentum theory, using the calculated value of the propeller thrust.

Figs. 8-9 show the convergence history of the non-dimensional lateral forces at the aft and fore part of the ship hull, respectively; excluding the mid part, for all test conditions, except Test2. The value of lateral forces depends on test conditions and ship geometry, but the force at the stern is strongly related to the propeller loading, also showing the blade passage frequency. The time history of the lateral forces at the ship bow shows that the converged value at the bow is shifted in time with respect to the stern, and this “shift time step” is also related to the advance ratio.

If $L_{PP}/(V_s + U_a/2)$ is the time unit needed by a fluid particle to go from the propeller plane to the end of ship bow if it had a constant velocity, then Fig. 9 shows that the lower the advance ratio is, the shorter the effective time is that is actually needed for the disturbance from the propeller to

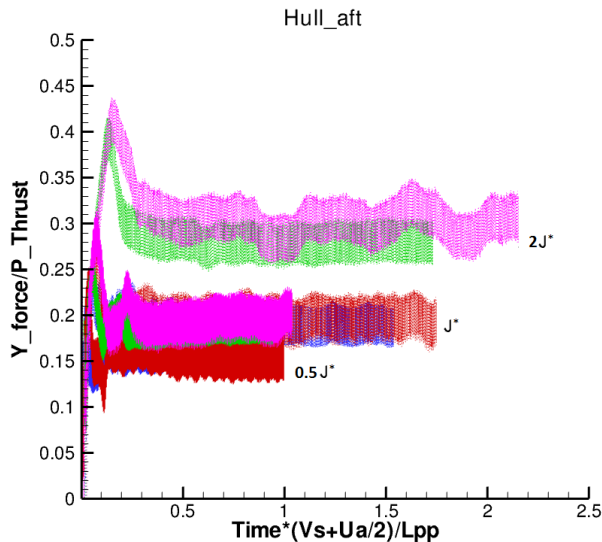


Figure 8: Convergence history of lateral force at the aft.

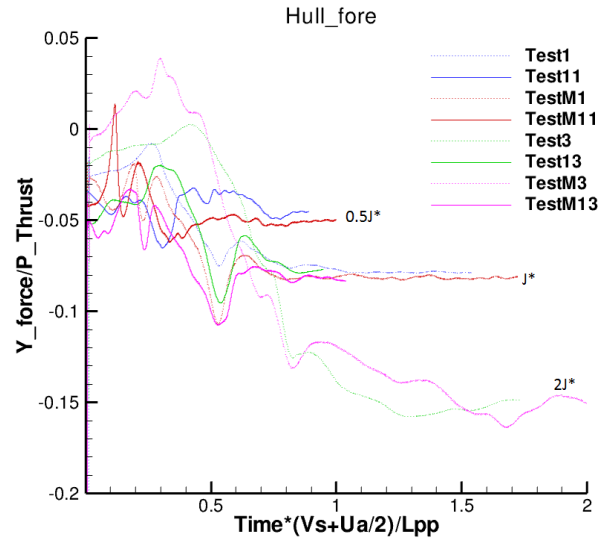


Figure 9: Convergence history of lateral force at the fore.

propagate downstream. This is because the acceleration of the fluid caused by the propeller is stronger and because the relative velocity of the propeller wake is higher with respect to the ship advance speed.

The converged (and averaged for the aft part) non-dimensional values of lateral forces and total turning moment for all the test conditions are reported in Fig. 10. The strong correlation between the advance ratio J and the lateral forces experienced by the ship hull and the total yaw moment is evident. They all increase (in absolute value) when increasing the advance ratio. It is worth noting that Test13 and TestM1 have nothing in common but the advance ratio J^* and they experience the same lateral forces at the bow and at the stern and the same total turning moment, in terms of non-dimensional results.

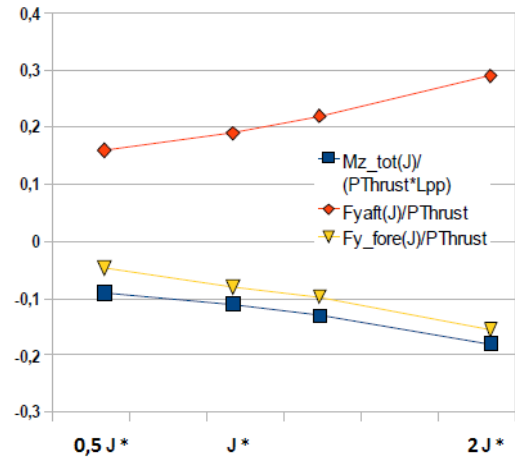


Figure 10: Non-dimensional side forces on the ship hull and total turning moment as function of the advance ratio J .

Test1 is the case with the largest value of turning moment. In Fig. 11 the reduction of the total turning moment, calculated with respect to the Test1 conditions, shows how it decreases, in the absolute value, when decreasing the ship negative advance speed, the propeller thrust, and the ship length.

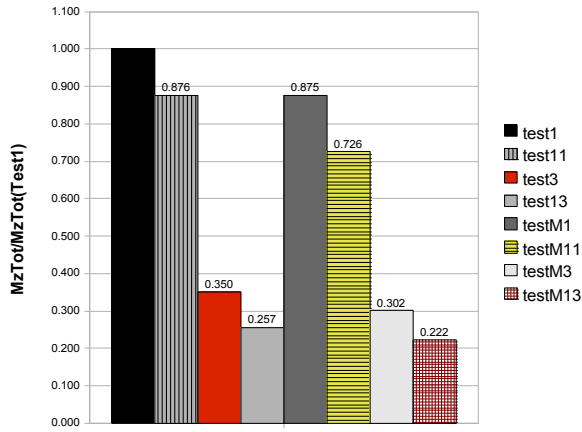


Figure 11: Reduction of total turning moment obtained reducing propeller revolutions, and/or velocity ship advance and/or ship length.

6 MODEL IMPLEMENTATION IN SHIP SIMULATOR

For the specific use of these results in a ship simulator, it is preferable to focus on the ship hull only and to represent the turning moment acting on it, in terms of side forces and their application point on the hull. In fact, specific models for propeller and rudder are usually available in ship simulators.

It is important to highlight that in the previous section the total turning moment on the model was described, also including the contributions from propeller unit and rudder, and that the side forces were obtained only integrating over the parts of the hull which are unchanged in the two models with different ship length. For this purpose, the yaw moment has been recalculated on the hull only by simply discarding the contribution from the rudder propeller, and the side forces are also integrated considering the middle part of the hull, which is different in the two models.

This will not substantially change the results as described above, mainly because the contributions in terms of side forces from the propeller unit are small if compared to the side forces acting on the hull. The same evaluation also applies to the mid-hull, where the side forces are small in the original model and negligible for the modified ship length. Fig. 12 shows how the model has been decomposed in different parts, and Fig. 13 shows an example of results for Test11 and TestM11 reporting the contributions deriving from each part in terms of non-dimensional side forces during a single propeller revolution.

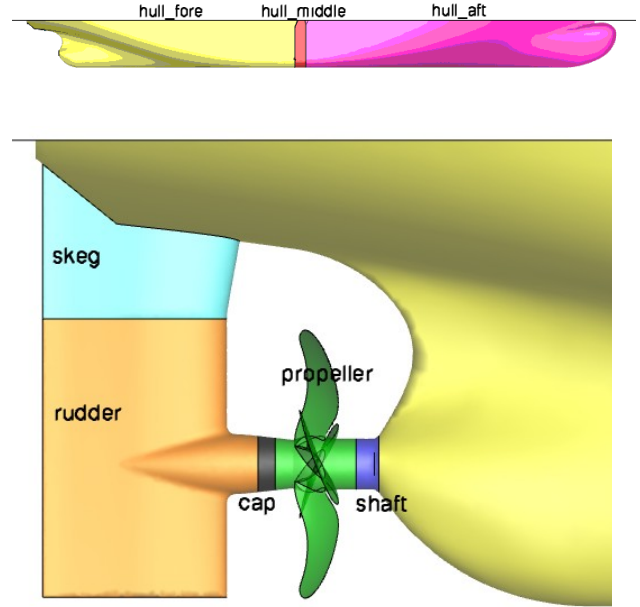
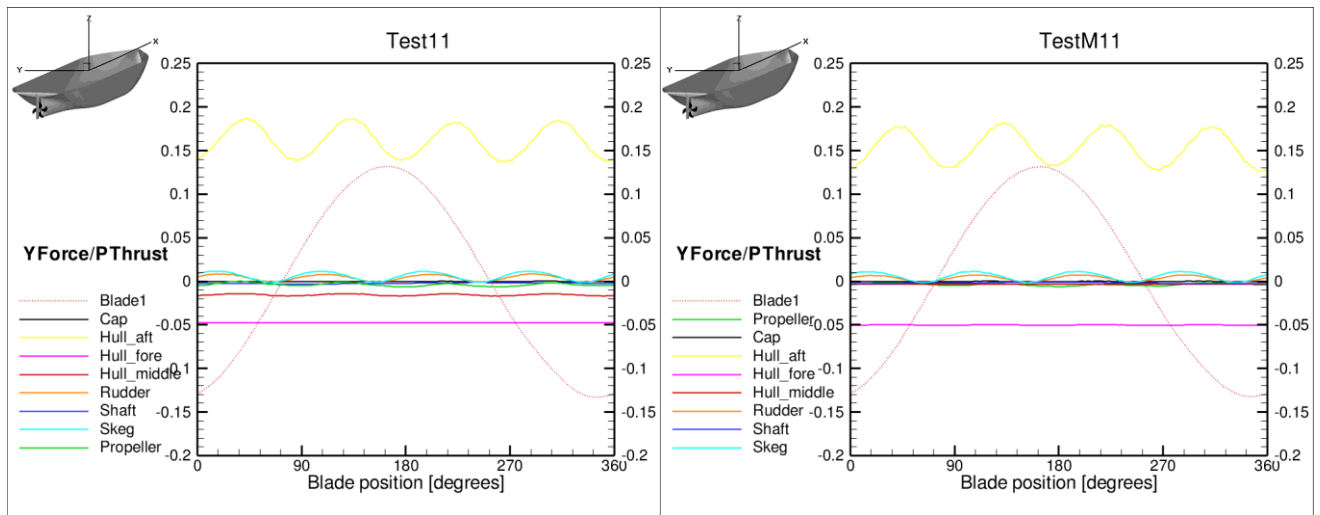


Figure 12: Identification of different parts of the model (modified model). The original model only differs in the middle part of the hull.



(a)

(b)

Figure 13: Non-dimensional side forces on the different parts of the model as function of the blade position, during a single propeller revolution. Test11 (a) and TestM11 (b).

The variables of interest, i.e., the side forces and their arms, in non-dimensional form are still dependent from the advance ratio J , as shown in Figs. 14-15. The ship length is only slightly affecting the forces and application points, mainly at the bow. According to the applied reference system, the X-coordinate for the application point at the aft is negative, while it is positive for the forebody with respect to the pivot point located at $L_{pp}/2$. The non-dimensional side forces, both at the aft and at the fore, increase in absolute value when increasing the advance ratio. The application point of the side force at the aft is always located at $0.5 \cdot L_{pp}$ from the pivot point,

while the application point at the fore moves downstream, toward bow when the advance ratio J increases.

Numerical models have been obtained to express the indirect transverse forces at the fore and at the aft of the ship, and their application points as a function of the advance ratio J . From them, the yaw moment can be calculated. According to the sign conventions used in the report, the yaw moment experienced by the hull is negative in this case. It is proportional to the ship length and to the propeller loading, and it is function of the advance ratio.

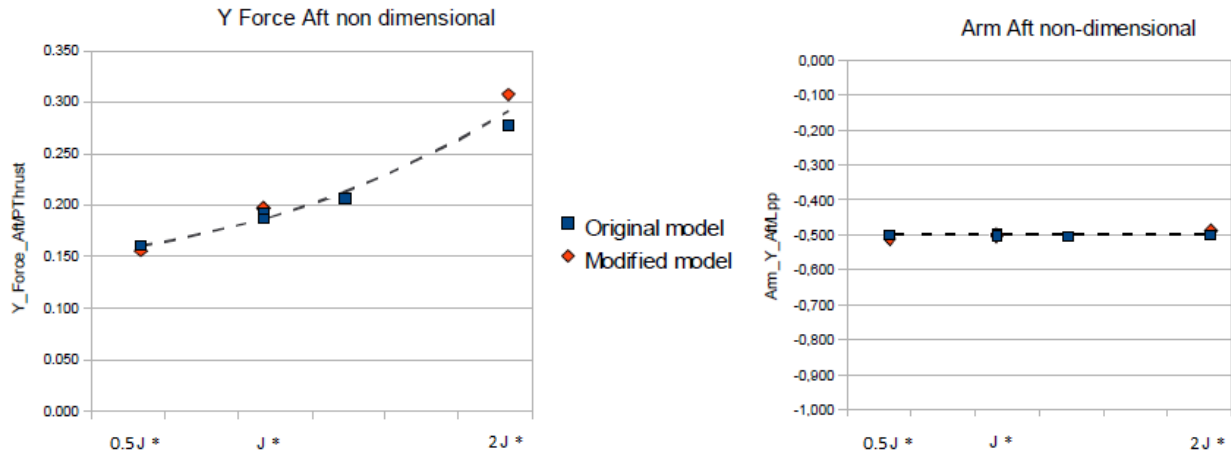


Figure 14: Side forces and application points on the aft part of the hull.

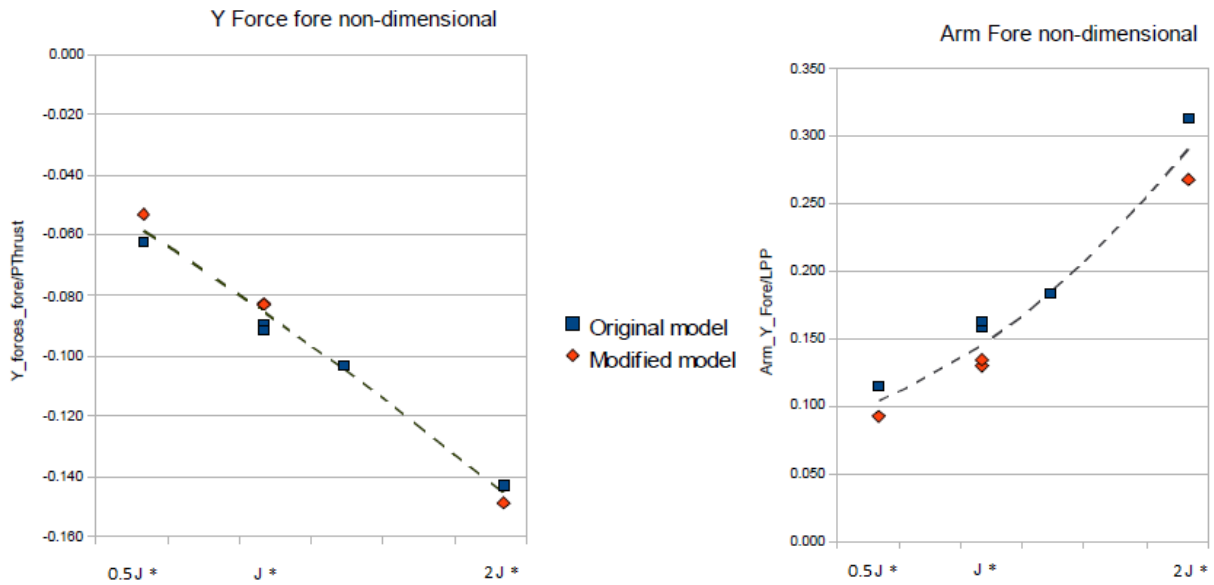


Figure 15: Side forces and application points on the fore part of the hull.

7 CONCLUSIONS

In the current work, forces and turning moments experienced by a single-screw ship model in reversing mode are investigated, both with model tests and RANS methods. Comparison of model tests and calculations shows that numerical results are in good agreement with experiments. The CFD results clearly show how transverse forces of opposite directions are generated at the stern and bow in accordance to model tests, and that the side force generated in the bow is delayed in time relative to the force in the stern when the propeller speed is suddenly changed. Additional numerical tests on a modified ship model show that the yaw moment is increasing with increasing ship length, while the side forces are less affected.

In terms of non-dimensional forces and moments, the most important parameter is the advance ratio J . Models with different ship lengths experience the same transverse forces at the ship bow and stern and the same total turning moment in terms of non-dimensional results if the same advance ratio is applied, also considering different propeller revolution rate and ship advance speed.

A mathematical model has been obtained which is able to express the non-dimensional lateral forces, their application points and the resulting yaw moment on the hull as functions of the advance ratio J . The model coefficients may probably change when modifying the ship hull form and/or the propeller unit. It is possible to check this by repeating the simple experimental investigation reported here with other ship and propeller

models. This might also be done using CFD, but when the model is mounted in the tank for doing self-propulsion tests, adding extra reversing tests is quick and adds very little to the cost.

The aim of the present work is to provide data and physical understanding for development of a simplified model, suited for implementation in a real-time ship simulator.

ACKNOWLEDGEMENT

This work has been performed within the Roll-Royce University Technology Centre 'Performance in a Seaway' at NTNU, in Trondheim. The authors wish to thank Roll-Royce Marine for permission to publish the paper. Special thanks are given to Marintek for providing the model test data.

This project was partially supported by the Norwegian HPC project NOTUR that granted access to its computer facilities.

REFERENCES

- Brix, J. (ed.) (1993). Manoeuvring Technical Manual. Seehafen Verlag GmbH.
- Fluent. (2006). Fluent 6.3 User Guide. Fluent Inc.
- Menter, F. R. (1994). 'Two-equation eddy-viscosity turbulence modeling for engineering applications'. AIAA Journal **32**(8) pp. 1598-1605.